

Two methods for measuring Bell nonlocality via local unitary invariants of two-qubit systems in Hong-Ou-Mandel interferometers

Karol Bartkiewicz^{1,2,*} and Grzegorz Chiriac¹

¹*Faculty of Physics, Adam Mickiewicz University, PL-61-614 Poznań, Poland*

²*RCPTM, Joint Laboratory of Optics of Palacký University and
Institute of Physics of Academy of Sciences of the Czech Republic,
17. listopadu 12, 772 07 Olomouc, Czech Republic*

(Dated: November 16, 2018)

We describe a direct method to experimentally determine local two-qubit invariants by performing interferometric measurements on multiple copies of a given two-qubit state. We use this framework to analyze two different kinds of two-qubit invariants of Makhlin and Jing et. al. These invariants allow to fully reconstruct any two-qubit state up to local unitaries. We demonstrate that measuring 3 invariants is sufficient to find, e.g., the optimal Bell inequality violation. These invariants can be measured with local or nonlocal measurements. We show that the nonlocal strategy that follows from Makhlin's invariants is more resource-efficient than local strategy following from the invariants of Jing et al. To measure all of the Makhlin's invariants directly one needs to use both two-qubit singlet and three-qubit W -state projections on multiple copies of the two-qubit state. This problem is equivalent to a coordinate system handedness measurement. We demonstrate that these 3-qubit measurements can be performed by utilizing Hong-Ou-Mandel interference which gives significant speedup in comparison to the classical handedness measurement. Finally, we point to potential application of our results in quantum secret sharing.

PACS numbers: 03.67.Mn, 42.50.Dv

I. INTRODUCTION

Local unitary invariants are fundamental quantities that do not change after performing local unitary transformations on subsystems of a composite quantum system [1–5]. In a way they are similar to constants of motion in classical mechanics, which remain unchanged under some transformations performed locally on coordinate systems of its parts. The invariants are proved to be a useful and powerful mathematical tool that can be applied in designing and analyzing quantum gates [3, 6], quantum error correction [7] and for measuring quantum correlations [8–11]. In this paper, we focus on a two-qubit case, which is especially important for practical applications as two-qubit correlations are necessary for performing various quantum information processing and quantum communications tasks that rely on quantum entanglement [12–14]. These applications include, e.g., dense coding [15], quantum teleportation [16], entanglement swapping [17], entanglement-based quantum key distribution [18, 19], quantum repeaters [20], quantum nondemolition photon detection [21, 22] used for qubit amplification [23]. Moreover, the quantum correlations can be interpreted as a manifestation of nonlocality and detected by breaking the Bell-Cluser-Horne-Shimony-Holt inequality [24–27].

Here, we demonstrate that local invariants are not only a convenient tool to analyze these phenomena, but also they can be used to design new experiments for measur-

ing quantum correlations and other nonlinear properties of quantum states (like, e.g., nonlocality). For this purpose we focus on two sets of local unitary invariants, i.e., Makhlin's invariants I from Ref. [3] and invariants of Jing et al. J from Ref. [5]. We show that all the investigated invariants can be expressed as expected values of measurements performed on multiple copies of a given two-qubit system. Hence, each invariant can be expressed as a combination of measurements with outcomes valued ± 1 . We group these composite measurements in three categories, i.e., local chained, local looped, and nonlocal measurements shown in Figs. 1-3. The local measurements are invariant under local unitaries and their prime element is a singlet projection, which is naturally implemented in linear optical systems by measuring anticorrelation rate of photons that interfered on a balanced beam splitter, i.e., by measuring Hong-Ou-Mandel (HOM) interference [28]. Similar composite HOM measurements were used in several experimental and theoretical works related to detecting and measuring, e.g., quantum entanglement, quantum discord, purity of quantum states, and performing optimal quantum tomography or measuring spectra of density matrices (see, e.g., Refs. [10, 11, 29–43]). The vast subject of multiphoton interferometry is reviewed in Ref. [44]. Here, we show that some of the most complex Makhlin's invariants [3] can be expressed by projections on 3 particle W -states, which do not exhibit bipartite entanglement [45]. The results of such measurements can be interpreted as measuring handedness of a coordinate system formed by three Bloch vectors. We demonstrate that even by using projections on maximally entangled two-qubit states it is possible to perform the handedness measurement much faster than by using

*Electronic address: bark@amu.edu.pl

the classical approach to the problem based on separable single-qubit projections.

In this paper, we describe two alternative ways of performing a test of Bell-Clauser-Horne-Shimony-Holt (Bell-CHSH) inequality violation [26] to the approaches known from the literature [26, 27, 33, 41, 43, 46–53]. Each of these methods is related to a different set of invariants and allows to directly test the optimal Bell-CHSH inequality and quantify the level of its violation. We also show that the presented interferometers can be also used for measuring the fully entangled fraction [54], which is useful for estimating the fidelity of many entanglement-based quantum information protocols (see, e.g., Refs. [41, 54–57]).

This paper is organized as follows: In Sec. II, we establish the theoretical framework to be used for expressing the invariants I and J in terms of quantities which are measurable via HOM interference. In Sec. III, the Makhlin's and Jing's et al. invariants are defined via experimentally-accessible state projections. In Sec. IV we describe two new approaches towards measuring Bell-CHSH nonlocality and other quantities based on invariants I and J , e.g., fully-entangled fraction. We conclude in Sec. V.

II. THEORETICAL FRAMEWORK

A. Two-qubit density matrix

A two-qubit density matrix can be represented in standard Hilbert-Schmidt form using Einstein's summation convention as

$$\hat{\rho}_{a,b} = \left(\frac{1}{4} \hat{\sigma}_0^{\otimes 2} + s_i \hat{\sigma}_i \otimes \hat{\sigma}_0 + p_i \hat{\sigma}_0 \otimes \hat{\sigma}_i + \beta_{i,j} \hat{\sigma}_i \otimes \hat{\sigma}_j \right)_{a,b}, \quad (1)$$

where in the case of photonic polarization qubits the Pauli matrices can be expressed in terms of projections on horizontal $|H\rangle$, vertical $|V\rangle$, diagonal $|D\rangle$, antidiagonal $|A\rangle$, left-circular $|L\rangle$, and right-circular $|R\rangle$ single-photon polarization states, i.e., as $\hat{\sigma}_0 = |H\rangle\langle H| + |V\rangle\langle V|$, $\hat{\sigma}_1 = |D\rangle\langle D| - |A\rangle\langle A| \equiv \hat{\sigma}_x$, $\hat{\sigma}_2 = |L\rangle\langle L| - |R\rangle\langle R| \equiv \hat{\sigma}_y$, and $\hat{\sigma}_3 = |H\rangle\langle H| - |V\rangle\langle V| \equiv \hat{\sigma}_z$. The photons observed individually have Bloch vectors \mathbf{s} and \mathbf{p} for subsystems in modes a and b , respectively. The correlations between the subsystems are described by matrix $\hat{\beta}$.

B. Singlet projections

Projections on singlet state are often implemented in studying quantum aspects of polarization-encoded two-qubit state and as an element of such quantum information processing task as, e.g., quantum teleportation, entanglement swapping, and dense coding etc. The singlet projection can be implemented by a balanced beam splitter (BS), which performs the following operations on the Bell basis states [i.e., $|\Psi^\pm\rangle = \frac{1}{\sqrt{2}}(|HV\rangle \pm |VH\rangle)$ and

$|\Phi^\pm\rangle = \frac{1}{\sqrt{2}}(|HH\rangle \pm |VV\rangle)$] of pairs of photons in spatial modes k and l

$$\begin{aligned} \hat{U}_{\text{BS}}|\Psi^-\rangle_{k,l} &= -|\Psi^-\rangle_{k,l} = -\frac{1}{\sqrt{2}}(|H,V\rangle - |V,H\rangle)_{k,l} \\ \hat{U}_{\text{BS}}|\Psi^+\rangle_{k,l} &= \frac{1}{\sqrt{2}}(|HV,0\rangle - |0,HV\rangle)_{k,l} \\ \hat{U}_{\text{BS}}|\Phi^\pm\rangle_{k,l} &= \frac{1}{2}(|2H,0\rangle - |0,2H\rangle)_{k,l} \\ &\quad \pm \frac{1}{2}(|2V,0\rangle - |0,2V\rangle)_{k,l}, \end{aligned} \quad (2)$$

where $|0\rangle$ is the vacuum, $|V,H\rangle_{k,l} = \hat{b}_{k,V}^\dagger \hat{b}_{l,H}^\dagger |0,0\rangle$, and $|2V,0\rangle_{k,l} = \frac{1}{\sqrt{2}} \hat{b}_{k,V}^{\dagger 2} |0,0\rangle_{k,l}$, etc. These transformations can be derived in the Heisenberg picture with input and output annihilation operators for polarization $p = H, V$ are $\hat{a}_{k,p}$, $\hat{a}_{l,p}$ and $\hat{b}_{k,p}$, $\hat{b}_{l,p}$, respectively. For this BS the input-output relations read as $\hat{a}_{k,p} = (\hat{b}_{k,p} + \hat{b}_{l,p})/\sqrt{2}$ and $\hat{a}_{l,p} = (\hat{b}_{k,p} - \hat{b}_{l,p})/\sqrt{2}$. Thus, if we detect at the same time one photon in each output of the BS, we perform the singlet projection. Similarly, if we detect two photons of orthogonal polarizations in a single output mode of the BS, we perform the $|\Psi^+\rangle_{k,l}$ state projection. In the latter case, one usually uses polarizing beam splitters (PBS).

It can be shown by direct calculations that a singlet projection

$$\hat{P}_{k,l}^- = \frac{1}{4} (2\hat{\sigma}_0 \otimes \hat{\sigma}_0 - \hat{\sigma}_i \otimes \hat{\sigma}_i)_{a,b} = (|\Psi^-\rangle\langle\Psi^-|)_{k,l} \quad (3)$$

performed on photons in modes k and l is equivalent to a two-particle observable $(\hat{\sigma}_i \otimes \hat{\sigma}_i)_{k,l} = \hat{\sigma}_0^{\otimes 2} - 4\hat{P}_{k,l}^-$ for particles k and l . This projection on a singlet state is graphically represented throughout this paper as a red curve (see Figs. 1-3). The multiple copies of a given two-qubit state are depicted as dashed lines with black and white ends representing the potentially quantum-correlated subsystems of Alice and Bob.

When we have access to multiple copies of the same bipartite system we can perform singlet projections between various qubits. However, not every possible sequence of projections is needed for determining the values of local invariants. These sequences depend on the particular invariants. For the invariants discussed in this paper we can group the possible sets of projections into local chained projections (singlet projections are performed only locally, see Fig. 1), local looped projections (similar as chained projections, but all qubits are paired, see Fig. 2), and nonlocal projections (singled projections made on systems that are locally separated, see Fig. 3). We will demonstrate that, if we analyze only J invariants [5] we do not need to apply the nonlocal projections.

Note that some of the projections shown in Figs. 1–3 require a high number of copies of a given two-qubit state and performing experiments with a large number of photon pairs may be very challenging [44]. However, there are experimental works using multiple copies of a two-qubit state to measure nonlinear properties of the quantum system [29, 41, 42].

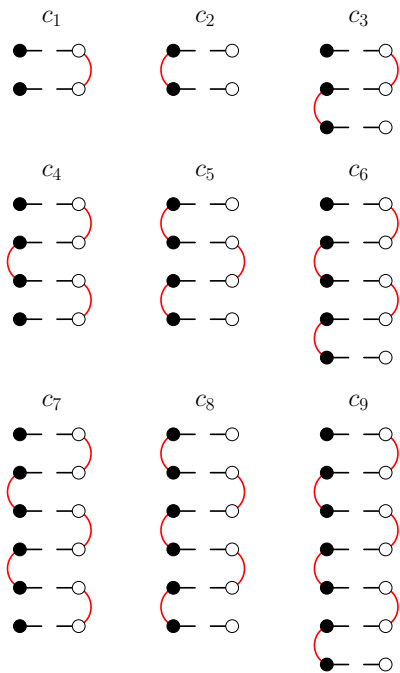


FIG. 1: Local chained singlet projection measurements. With each label we associated a probability of projecting the multicopy system onto singlets (red curves), i.e., HOM anticorrelation. This notation is used for expressing both Makhlin's and Jing's invariants in terms of multicopy singlet projections. Note that every low rank composite singlet projection can be observed as an invariant in a more complex interferometer designed to measure a higher rank chained singlet projection.

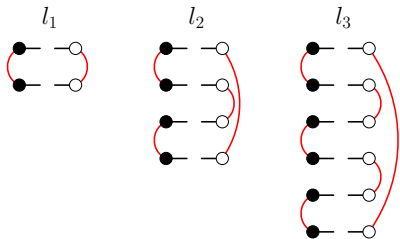


FIG. 2: The same as in Fig. 1 but for looped singlet measurement sequences. Note that all measurement corresponding to diagrams from c_1 to c_8 can be implemented by an interferometer designed for measuring one of the looped diagrams l_n for $n = 1, 2, 3$.

C. Reducing W -state projection to singlet projections

The second prime measurement that appears in the most complex of Makhlin's invariants is a three-particle observable

$$\hat{W}_{k,l,m} = (|W_0\rangle\langle W_0| + |W_1\rangle\langle W_1| - |W_2\rangle\langle W_2| - |W_3\rangle\langle W_3|)_{k,l,m}, \quad (4)$$

where $|W_0\rangle_{k,l,m} = (|HHV\rangle + e^{i2\pi/3}|HVV\rangle + e^{i4\pi/3}|VHH\rangle)_{k,l,m}/\sqrt{3}$, $|W_1\rangle_{k,l,m} = (|VVH\rangle +$

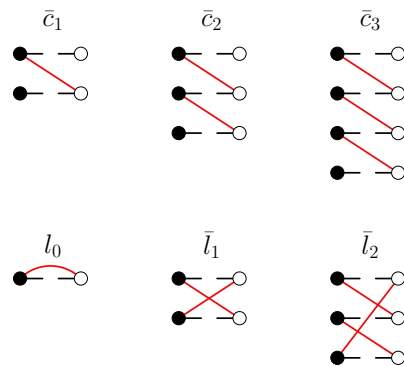


FIG. 3: Nonlocal chained and looped singlet projection operations. With each label we associated a probability of projecting the multicopy system onto singlets (red curves). This notation is used for expressing both Makhlin's invariants in terms of multicopy singlet projections. Note that measurements \bar{c}_1 and \bar{c}_2 can be performed in interferometers designed for measuring \bar{l}_1 (only \bar{c}_1) or \bar{l}_2 .

$e^{i2\pi/3}|VHV\rangle + e^{i4\pi/3}|HVV\rangle)_{k,l,m}/\sqrt{3}$, $|W_2\rangle_{k,l,m} = (|HHV\rangle + e^{-i2\pi/3}|HVV\rangle + e^{-i4\pi/3}|VHH\rangle)_{k,l,m}/\sqrt{3}$, $|W_3\rangle_{k,l,m} = (|VVH\rangle + e^{-i2\pi/3}|VHV\rangle + e^{-i4\pi/3}|HVV\rangle)_{k,l,m}/\sqrt{3}$, are W -states that manifest only tripartite entanglement. This observable emerges while dealing with determinants of matrices formed by 3 Bloch vectors describing qubits in modes k, l, m , i.e., $\hat{W}_{k,l,m} = e_{r,s,t}(\hat{\sigma}_r \otimes \hat{\sigma}_s \otimes \hat{\sigma}_t)_{k,l,m}$. It is interesting that this measurement quantifies the imbalance between the probabilities of 3-qubit state belonging to two subspaces (one spanned by $|W_0\rangle_{k,l,m}, |W_1\rangle_{k,l,m}$ and the other by $|W_2\rangle_{k,l,m}, |W_3\rangle_{k,l,m}$) being complex conjugates of themselves. The complex conjugation of a state is associated with time reversal symmetry and $\hat{W}_{k,l,m}$ measurements break this symmetry. Thus, such a measurement can discriminate spins rotating in the opposite directions. This measurement can be also interpreted as a way of distinguishing left-handed and right-handed coordinate system formed by Bloch vectors corresponding to the 3 measured qubits. This is a simple example of quantum supremacy, where a projection on an entangled state provides an answer to the stated problem (calculating an arbitrary 3 dimensional determinant) much faster than the classical analysis. Note that there is an elegant method of projecting a 3-photon state on a W -state [58–60]. However, this method works with limited probability and would not allow us to distinguish between the pair of states ($|W_0\rangle_{k,l,m}, |W_1\rangle_{k,l,m}$) and ($|W_2\rangle_{k,l,m}, |W_3\rangle_{k,l,m}$).

It turns out that we can implement the W -state projection by HOM interference by using its alternative representation, i.e.,

$$\hat{W}_{k,l,m} = \hat{w}_{k,l,m} + \hat{w}_{l,m,k} + \hat{w}_{m,k,l} \quad (5)$$

projection with 3 configurations of HOM interferometer

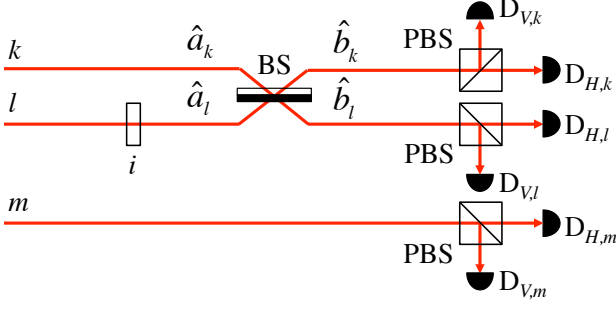


FIG. 4: Optical circuit for implementing linear-optical measurement of observable $\hat{w}_{k,l,m}$ given in Eq. (6). The circuit implement is composed of a $\pi/2$ phase shift corresponding to a phase factor i , a balanced beam splitter (BS) described by Eq. (2), polarizing beam splitters (PBSs), and detectors $D_{p,n}$ that count photons of polarization $p = H, V$ in spatial modes $n = k, l, m$. This circuit registers the outcome $+1$ if the following triples of detectors register a photon each, i.e., $(D_{V,k}, D_{H,k}, D_{V,m})$, $(D_{V,l}, D_{H,l}, D_{V,m})$, $(D_{V,k}, D_{H,l}, D_{H,m})$, and $(D_{H,k}, D_{V,l}, D_{V,m})$. Similarly, it registers -1 for the triples $(D_{V,k}, D_{H,k}, D_{H,m})$, $(D_{V,l}, D_{H,l}, D_{H,m})$, $(D_{V,k}, D_{H,l}, D_{V,m})$, and $(D_{H,k}, D_{V,l}, D_{H,m})$. The other possible detection events are associated with value 0.

using the circuit depicted in Fig. 4, where

$$\hat{w}_{k,l,m} = \left[2\hat{S}(|\Psi^-\rangle\langle\Psi^-| - |\Psi^+\rangle\langle\Psi^+|)\hat{S}^\dagger \otimes \hat{\sigma}_z \right]_{k,l,m} \quad (6)$$

for photons in spatial modes k, l, m and where $\hat{S} = \text{diag}[1, 1, i, i]$ is a single-qubit phase gate. This measurement reveals an interesting feature of quantum physics. By interference we can learn about the mutual orientation of three real (Bloch) vectors (decide if they are ordered in a way that form left or right-handed system) in only three measurements. Using a direct approach one has to measure all 3 components of all 3 vectors (i.e., 9 measurements in total in the general case of quantum correlated 3-qubit state). Thus, in this case we deal with quadratic speed-up. If one could measure the W -state projections directly, this speed up would be even greater.

III. LOCAL UNITARY INVARIANTS OF TWO-QUBIT STATES

A. Makhlin's Invariants

The invariants described by Makhlin in Ref. [3] can be expressed in terms of the correlation matrix $\hat{\beta} = \text{tr}[(\hat{\sigma}_i \otimes \hat{\sigma}_j)\hat{\rho}]$, and the Bloch vectors $\mathbf{s} = \text{tr}[(\hat{\sigma}_i \otimes \hat{\sigma}_0)\hat{\rho}]$ and $\mathbf{p} = \text{tr}[(\hat{\sigma}_0 \otimes \hat{\sigma}_j)\hat{\rho}]$. The matrices $\hat{\sigma}_i$ for $i = 0, 1, 2, 3$ are the Pauli matrices with $\hat{\sigma}_0$ being the single-qubit identity matrix. These invariants [3] are given as $I_1 = \det \hat{\beta}$, $I_2 = \text{tr}(\hat{\beta}^T \hat{\beta})$, $I_3 = \text{tr}(\hat{\beta}^T \hat{\beta}^2)$, $I_4 = \mathbf{s}^2$, $I_5 = [\mathbf{s}\hat{\beta}]^2$, $I_6 = [\mathbf{s}\hat{\beta}\hat{\beta}^T]^2$, $I_7 = \mathbf{p}^2$, $I_8 = [\hat{\beta}\mathbf{p}]^2$, $I_9 = [\hat{\beta}^T \hat{\beta}\mathbf{p}]^2$,

$I_{10} = (\mathbf{s}, \mathbf{s}\hat{\beta}\hat{\beta}^T, \mathbf{s}[\hat{\beta}\hat{\beta}^T]^2)$, $I_{11} = (\mathbf{p}, \hat{\beta}^T \hat{\beta}\mathbf{p}, [\hat{\beta}^T \hat{\beta}]^2 \mathbf{p})$, $I_{12} = \mathbf{s}\hat{\beta}\mathbf{p}$, $I_{13} = \mathbf{s}\hat{\beta}\hat{\beta}^T \hat{\beta}\mathbf{p}$, $I_{14} = e_{ijk}e_{lmn}s_i p_l \hat{\beta}_{jm} \hat{\beta}_{kn}$, $I_{15} = (\mathbf{s}, \mathbf{s}\hat{\beta}\hat{\beta}^T, \hat{\beta}\mathbf{p})$, $I_{16} = (\mathbf{s}\hat{\beta}, \mathbf{p}, \hat{\beta}^T \hat{\beta}\mathbf{p})$, $I_{17} = (\mathbf{s}\hat{\beta}, \mathbf{s}\hat{\beta}\hat{\beta}^T \hat{\beta}, \mathbf{p})$, $I_{18} = (\mathbf{s}, \hat{\beta}\mathbf{p}, \hat{\beta}\hat{\beta}^T \hat{\beta}\mathbf{p})$. Here $(\mathbf{a}, \mathbf{b}, \mathbf{c})$ stands for the triple scalar product $\mathbf{a} \cdot (\mathbf{b} \times \mathbf{c})$ and e_{ijk} is the Levi-Civita symbol.

As shown in Ref. [43], the Makhlin's invariants relevant to measuring entanglement in terms of negativity are as follows

$$\begin{aligned} I_1 &= -\frac{8}{3}\{l_0[l_0(4l_0 - 3) + 6(\bar{c}_1 - 2\bar{l}_1)] \\ &\quad + 3\bar{l}_1 - 6\bar{c}_2 + 8\bar{l}_2\}, \\ I_2 &= 1 + 16l_1 - 4(c_2 + c_1), \\ I_3 &= 1 + 256(c_2^2 + 4c_3 + c_1^2 + l_2) - 8(c_2 + c_1) \\ I_4 &= 1 - 4c_2, \\ I_5 &= -4c_1 + 32c_3 - 64c_5 + (1 - 4c_2)^2, \\ I_7 &= 1 - 4c_1, \\ I_8 &= -4c_2 + 32c_3 - 64c_4 + (1 - 4c_1)^2, \\ I_{12} &= 1 + 16c_3 - 4(c_2 + c_1), \\ I_{14} &= 16[l_0^2(1 - 4\bar{c}_1) + 2l_0(4\bar{c}_2 - \bar{c}_1) \\ &\quad - \bar{l}_1 + 4\bar{c}_1\bar{l}_1 + 2\bar{c}_2 - 8\bar{c}_3], \end{aligned} \quad (7)$$

where the relevant 13 terms $l_0, c_2, \bar{c}_1, c_1, l_1, c_3, \bar{l}_1, \bar{c}_2, \bar{l}_2, c_5, c_4, l_2, \bar{c}_3$, are singlet projections depicted in Figs. 1–3 and can be measured utilizing only HOM interference. Similarly, we find the following 3 of the remaining invariants

$$\begin{aligned} I_6 &= 1 - 1024c_8 - 4(3c_2 + 2c_1) \\ &\quad + 16(3c_2^2 + 4c_3 + 2c_2c_1 + c_1^2) \\ &\quad - 64(c_2^3 + 4c_2c_3 + 2c_5 + 2c_3c_1 + c_4) \\ &\quad + 256(c_3^2 + 2c_2c_5 + 2c_6) \\ I_9 &= 1 - 1024c_7 - 4(2c_2 + 3c_1) \\ &\quad + 16(c_2^2 + 4c_3 + 2c_2c_1 + 3c_1^2) \\ &\quad - 64(2c_2c_3 + c_5 + 4c_3c_1 + c_1^3 + 2c_4) \\ &\quad + 256(c_3^2 + 2c_6 + 2c_1c_4), \\ I_{13} &= 1 + 256c_6 - 8(c_2 + c_1) \\ &\quad + 16(c_2^2 + 3c_3 + c_2c_1 + c_1^2) \\ &\quad - 64[c_5 + c_3(c_2 + c_1) + c_4], \end{aligned} \quad (8)$$

that can be measured using very similar interferometers composite HOM to these described in Ref. [43]. These can be designed as explained in Ref. [43], i.e., by constructing interferometers that would at best (if all the detector pairs detect anticoalescence) measure the values of c_7 or c_8 , and for other combinations of anticoalescence and coalescence events would measure polynomials of c_n for $n = 1, 2, 3, 4, 5, 6$. The remaining six remaining invariants I_n for $n = 10, 11, 15, 16, 17, 18$ require a new approach. These six invariants are needed only to bound the signs of the components of the \mathbf{s} and \mathbf{p} vectors. Thus, their absolute values are not important. We cannot measure them directly only with HOM interference limited only to coalescence and anticoalescence detection. This is because in order to estimate the value

of a three-particle observable $\langle e_{ijk} \hat{\sigma}_i \otimes \hat{\sigma}_j \otimes \hat{\sigma}_k \rangle_{k,l,m}$ for particles k, l , and m one needs to measure $\hat{W}_{k,l,m}$ defined in Eq. (4). The physical interpretation of this \hat{W} measurement is the difference of the probabilities of Bloch vectors of the three qubits forming left-hand and right-hand coordinate system. If one performs only the anticoalescence detection, at best one measures $\hat{W}_{k,l,m}^2 = \sum_{n=0,1,2,3} |W_n\rangle \langle W_n|_{k,l,m} = P_{k,l} + P_{k,m} + P_{l,m}$, which does not break the time reversal symmetry. Hence, only with simple interferometers we can measure only I_n^2 for $n = 10, 11, 15, 16, 17, 18$, where the sign is lost and it makes the invariants useless. However, \hat{W} measurement can be performed indirectly as explained by Eq. (6) and in Fig. 4.

It is very interesting to observe that one would need three-particle measurements to measure directly some of the local two-particle invariants. However, these handedness invariants are special as they reveal mutual orientation of the Bloch vector components of the subsystems of density matrix $\hat{\rho}$ (i.e., the signs of s_i, p_i for $i = 1, 2, 3$) [3], while other I invariants could be used only to determine the absolute values. Thus, any locally invariant properties of a two-qubit state can be assessed by using only singlet and W -state projections on multiple copies of the two-qubit system. The latter can be expressed by modified $|\Psi^\pm\rangle$ projections and $\hat{\sigma}_z$ measurements as shown in Eq (6). Hence, we can measure the J invariants with only HOM interference and $\hat{\sigma}_z$ measurement. The exact experimental procedure for measuring invariants I_n for $n = 10, 11, 15, 16, 17, 18$ is straightforward, but it would take much space to cover in detail. For sake of clarity of the paper we list only the partial observations needed for such measurements within the above-described framework in Appendix A. All these observations are local.

B. Jing's et al. invariants

It turns out that we do not need W state measurement or $\hat{\sigma}_z$ to check if a two two-qubit states are equivalent up to local unitaries. Remarkably it was shown by Jing et al. [5] that there are 12 local invariants that are equivalent to the set of 18 Makhlin's invariants. This means that both sets of invariants are sufficient to decide if any pair of two-qubit states is locally equivalent. The 6 Makhlin's invariants I_n for $n = 10, 11, 15, 16, 17, 18$ are inequivalent to trivial polynomials of Jing's invariants, as at the most fundamental level they cannot be reduced to simple singlet projections on multiple copies. However, we find that Jing's invariants can be related to other Makhlin's

invariants via singlet projections in the following way

$$\begin{aligned}
 J_1 &= \text{tr}(\hat{\beta}^T \hat{\beta}) = I_2, \\
 J_2 &= \text{tr}(\hat{\beta}^T \hat{\beta})^2 = I_3, \\
 J_3 &= \text{tr}(\hat{\beta}^T \hat{\beta})^3 = \frac{1}{2}(6I_1^2 - I_2^3 + 3I_2 I_3), \\
 J_4 &= \mathbf{s}^2 = I_4, \\
 J_5 &= [\mathbf{s} \hat{\beta}]^2 = I_5, \\
 J_6 &= [\mathbf{s} \hat{\beta} \hat{\beta}^T]^2 = I_6, \\
 J_7 &= \mathbf{p}^2 = I_7, \\
 J_8 &= [\hat{\beta} \mathbf{p}]^2 = I_8, \\
 J_9 &= [\hat{\beta}^T \hat{\beta} \mathbf{p}]^2 = I_9, \\
 J_{10} &= \mathbf{s} \hat{\beta} \mathbf{p} = I_{12}, \\
 J_{11} &= \mathbf{s} \hat{\beta} \hat{\beta}^T \hat{\beta} \mathbf{p} = I_{13}, \\
 J_{12} &= \mathbf{s} \hat{\beta} \hat{\beta}^T \hat{\beta} \hat{\beta}^T \hat{\beta} \mathbf{p}.
 \end{aligned} \tag{9}$$

In particular we can also express J_3 and J_{12} as $J_3 = 4096l_3 - 3072(c_7 + c_8) + 768(2c_6 + c_4c_1 + c_5c_2 + c_3^2) - 64[3c_4 + 3c_5 + 6c_3(c_1 + c_2) + c_1^3 + c_2^3] + 48(2c_3 + c_1^2 + c_2^2 + c_1c_2) - 12(c_1 + c_2) + 1$ and $J_{12} = 4096c_9 - 1024(c_7 + c_8 + c_6c_1 + c_6c_2 + c_3c_4 + c_3c_5) + 768(3c_6 + c_4c_1 + c_5c_2 + c_3^2) - 64[2c_4 + 2c_5 + 6c_3(c_1 + c_2) + c_1^3 + c_2^3 + c_1^2c_2 + c_2^2c_1] + 16(5c_3 + 3c_1^2 + 3c_2^2 + 4c_1c_2) - 12(c_1 + c_2) + 1$, respectively. The interferometer for measuring J_{12} is equivalent to an interferometer designed for measuring c_9 in the case of detecting only anticoalescence events and other polynomials of c_n for $n = 1, 2, 3, 4, 5, 6, 7, 8$ for specific combinations of anticoalescence and coalescence events in the relevant detector pairs. Now we can make two interesting observations. Firstly, unlike the Makhlin's invariants all the invariants can be expressed by only local loops and chains. Secondly, note that the measurement of I_1 includes only nonlocal singlet projections which are fundamentally different from those which measure I_1^2 (only local singlet projections). This can be seen by expressing I_1^2 only by J_3, I_2 , and I_3 , which all three can be measured using only local singlet projections. The operational simplicity of J invariants has its price, but also some benefits. For example, due to the lost information about the sign of I_1 and no apparent way of extracting the value of I_{14} , we cannot calculate a value of negativity using solely J invariants. On the other hand, if one uses J invariants there is no need for performing \hat{W} measurement to check, if two states are equivalent up to local unitaries. Moreover, all the projections needed here are local. Hence, despite its benefits for verifying local equivalence of states, Jing's invariants appear to not be useful for measuring quantum entanglement (i.e., for measuring negativity we need both I_1 and I_{14} invariants that are measured via nonlocal measurements). However, still they can be applied to measuring nonlocality, as we demonstrate in the following section.

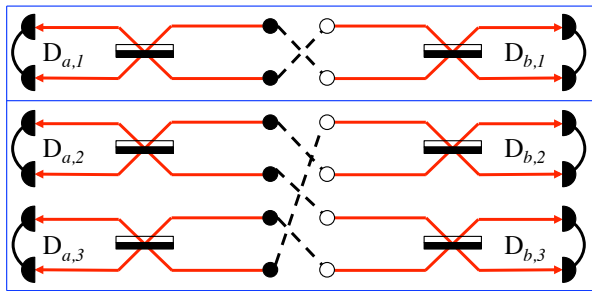


FIG. 5: Interferometric configurations for measuring two independent invariants I_2 and I_3 (or J_1 and J_2) associated with looped singlet projections l_1 and l_2 with two and four copies of polarization-encoded $\hat{\rho}$. Subsystems of a single copy are depicted as black and white discs connected with dashed lines. Photons interfere on beam splitters BS and their coalescence or anti-coalescence is detected by detector modules $D_{a,n}$ (Alice) and $D_{b,n}$ (Bob) for $n = 1, 2, 3$. For detailed analysis of all the possible detection events see Tab. I. To measure these invariant one needs to access at most 2 or 4 copies of the investigated state for I_2 and I_3 (or J_1 and J_2), respectively. All the measurements are local.

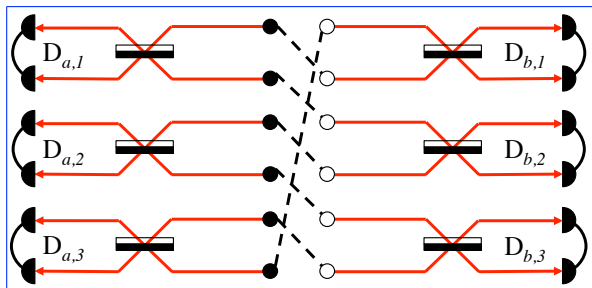


FIG. 6: Same as in Fig. 5, but for an interferometer measuring J_3 . To measure this invariant one needs to access 6 copies of the investigated state. For detailed analysis of all the possible detection events see Tab. II.

IV. TWO INVARIANT-BASED METHODS FOR MEASURING BELL-CHSH NONLOCALITY

Nonclassical correlations of polarizations can be measured by measuring only the eigenvalues of $\hat{R} = \hat{\beta}\hat{\beta}^T$ matrix. As it was experimentally demonstrated in Ref. [41], if one works with two copies of a density matrix, only six measurements are required to learn the eigenvalues r_n for $n = 1, 2, 3$. These eigenvalues can be used to express not only the maximal degree of Bell-CHSH inequality violation but also, e.g., fully-entangled fraction, and entropic entanglement witness for symmetric states [41]. The Horodecki measure of Bell (or CHSH) nonlocality can be expressed as [61]:

$$M = \text{Tr}\hat{R} - \min[\text{eig}(\hat{R})] - 1. \quad (10)$$

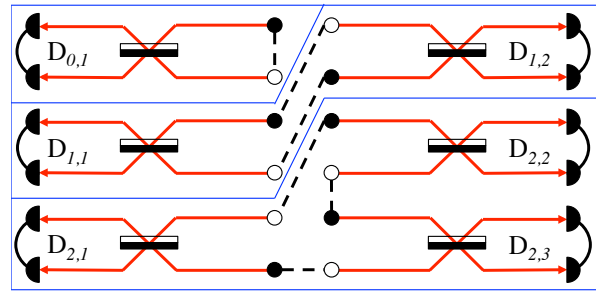


FIG. 7: Same as in Fig. 5, but for an interferometer measuring I_1 in terms of (from top) l_0 , \bar{l}_1 , and \bar{l}_2 . All the measurements are nonlocal (singlet projections are performed between subsystems of Alice and Bob). To measure this invariant one needs to access at most 3 copies of the investigated state. For detailed analysis of all the possible detection events see Tab. III.

TABLE I: Interpretation of detection events of the interferometers shown in Fig. 5. Each couple of detectors $D_{a,n}$ and $D_{b,n}$ for $n = 1, 2, 3$ detects coalesce or anti-coalescence for a pair of impinging photons. The accumulated counts of (anti-) coalescence events can be grouped into c coalescence or $s = a + c$ sum of coalescence (c) and anti-coalescence (a). The total number of all detection events in $D_{a,1}$ and $D_{b,1}$ is Z_1 . The remaining detection events accumulate to Z_2 . Depending on the measured quantity, one can choose the required detection events in accord with Fig. 1 or Fig. 2.

$D_{a,1}$	$D_{a,2}$	$D_{a,3}$	$D_{b,1}$	$D_{b,2}$	$D_{b,3}$	Fig. 5
s	-	-	s	-	-	Z_1
s	-	-	a	-	-	$Z_1 c_1$
a	-	-	s	-	-	$Z_1 c_2$
a	-	-	a	-	-	$Z_1 l_1$
-	s	s	-	s	s	Z_2
-	s	s	-	s	a	$Z_2 c_1$
-	s	s	-	a	s	$Z_2 c_1$
-	s	s	-	a	a	$Z_2 c_1^2$
-	s	a	-	s	s	$Z_2 c_2$
-	s	a	-	s	a	$Z_2 c_3$
-	s	a	-	a	s	$Z_2 c_3$
-	s	a	-	a	a	$Z_2 c_4$
-	a	s	-	s	s	$Z_2 c_2$
-	a	s	-	s	a	$Z_2 c_3$
-	a	s	-	a	s	$Z_2 c_3$
-	a	s	-	a	a	$Z_2 c_4$
-	a	a	-	s	s	$Z_2 c_2^2$
-	a	a	-	s	a	$Z_2 c_5$
-	a	a	-	a	s	$Z_2 c_5$
-	a	a	-	a	a	$Z_2 l_2$

TABLE II: The same as in Tab. I, but for an interferometer shown in Fig. 6

$D_{a,1}$	$D_{a,2}$	$D_{a,3}$	$D_{b,1}$	$D_{b,2}$	$D_{b,3}$	Fig. 6	$D_{a,1}$	$D_{a,2}$	$D_{a,3}$	$D_{b,1}$	$D_{b,2}$	$D_{b,3}$	Fig. 6
s	s	s	s	s	s	Z	a	s	s	s	s	s	Zc_2
s	s	s	s	s	a	Zc_1	a	s	s	s	s	a	Zc_2c_1
s	s	s	s	a	s	Zc_1	a	s	s	s	a	s	Zc_2c_1
s	s	s	s	a	a	Zc_1^2	a	s	s	s	a	a	$Zc_2c_1^2$
s	s	s	a	s	s	Zc_1	a	s	s	a	s	s	Zc_3
s	s	s	a	s	a	Zc_1^2	a	s	s	a	s	a	Zc_1c_3
s	s	s	a	a	s	Zc_1^2	a	s	s	a	a	s	Zc_4
s	s	s	a	a	a	Zc_1^3	a	s	s	a	a	a	Zc_1c_4
s	s	a	s	s	s	Zc_2	a	s	a	s	s	s	Zc_2^2
s	s	a	s	s	a	Zc_3	a	s	a	s	s	a	Zc_2c_3
s	s	a	s	a	s	Zc_3	a	s	a	s	a	s	Zc_2c_3
s	s	a	s	a	a	Zc_4	a	s	a	s	a	a	Zc_3^2
s	s	a	a	s	s	Zc_1c_2	a	s	a	a	s	s	Zc_2c_3
s	s	a	a	s	a	Zc_1c_3	a	s	a	a	s	a	Zc_6
s	s	a	a	a	s	Zc_1c_3	a	s	a	a	a	s	Zc_3^2
s	s	a	a	a	a	Zc_1c_4	a	s	a	a	a	a	Zc_3c_4
s	a	s	s	s	s	Zc_2	a	a	s	s	s	s	Zc_2^2
s	a	s	s	s	a	Zc_1c_2	a	a	s	s	s	a	Zc_2c_3
s	a	s	s	a	s	Zc_3	a	a	s	s	a	s	Zc_5
s	a	s	s	a	a	Zc_1c_3	a	a	s	s	a	a	Zc_6
s	a	s	a	s	s	Zc_3	a	a	s	a	s	s	Zc_2c_3
s	a	s	a	s	a	Zc_1c_3	a	a	s	a	s	a	Zc_3^2
s	a	s	a	a	s	Zc_4	a	a	s	a	a	s	Zc_6
s	a	s	a	a	a	Zc_1c_4	a	a	s	a	a	a	Zc_7
s	a	a	s	s	s	Zc_2^2	a	a	a	s	s	s	Zc_3^2
s	a	a	s	s	a	Zc_5	a	a	a	s	s	a	Zc_2c_5
s	a	a	s	a	s	Zc_2c_3	a	a	a	s	a	s	Zc_2c_5
s	a	a	s	a	a	Zc_6	a	a	a	s	a	a	Zc_8
s	a	a	a	s	s	Zc_2c_3	a	a	a	a	s	s	Zc_2c_5
s	a	a	a	s	a	Zc_3^2	a	a	a	a	s	a	Zc_8
s	a	a	a	a	s	Zc_1c_4	a	a	a	a	a	s	Zc_8
s	a	a	a	a	a	Zc_7	a	a	a	a	a	a	Zl_3

Its values are positive if the Bell-CHSH inequality is violated and it reaches the maximum $M = 1$ for maximally-entangled states. To express the fully-entangled fraction

$$f = \frac{1}{4} \left(\text{Tr} \sqrt{\hat{R}} + 1 \right), \quad (11)$$

which can be used to quantify the fidelity of many entanglement-based protocols [41, 55–57], one needs to calculate the square roots of the eigenvalues. Finally, the sum of eigenvalues of \hat{R} can be used directly to express the entropic entanglement witness E for equal purities of subsystems a and b (i.e., $\text{Tr} \rho_a^2 = \text{Tr} \rho_b^2$), and it reads as

$$E = 2(\text{Tr} \hat{\rho}_{a,b}^2 - \min[\text{Tr} \hat{\rho}_a^2, \text{Tr} \hat{\rho}_b^2]) = \frac{1}{2}(\text{Tr} \hat{R} - 1). \quad (12)$$

The measured value of this witness is positive, if it detects quantum entanglement and is negative otherwise. The

spectrum of \hat{R} can be calculated by measuring the first three invariants of Jing by applying only local projections or by measuring the first three invariants of Makhlin on fewer copies of the investigated state, but with using non-local projections. The spectrum of a three-dimensional matrix is given by the roots of the following polynomial in r in terms of J -invariants

$$-r^3 + J_1 r^2 + (J_1^2 - J_2)r + J_1^3 + 2J_3 - 3J_1 J_2 = 0 \quad (13)$$

or in terms of I -invariants

$$-r^3 + I_2 r^2 + (I_2^2 - I_3)r + I_2^3 + (6I_1^2 - I_2^3) = 0. \quad (14)$$

A similar approach can be used for determining eigenvalues of density matrices [38]. The specialized interferometers designed for measuring these projections are depicted in Figs. 5,6 and 5,7 for invariants J and I , respectively. The sets of projections necessary to determine

TABLE III: Same as in Tab. I, but for interferometers measuring nonlocal singlet projections from Fig. 3. Each couple of detectors $D_{0,1}$, $D_{1,1}$, $D_{1,2}$, and $D_{2,n}$, for $n = 1, 2, 3$ detects coalesce or anti-coalesce for a pair of impinging photons.

$D_{0,1}$	$D_{1,1}$	$D_{1,2}$	$D_{2,1}$	$D_{2,2}$	$D_{2,3}$	Fig. 7
s	-	-	-	-	-	Z_1
a	-	-	-	-	-	$Z_1 l_0$
-	s	s	-	-	-	Z_2
-	s	a	-	-	-	$Z_2 \bar{c}_1$
-	a	s	-	-	-	$Z_2 \bar{c}_1$
-	a	a	-	-	-	$Z_2 \bar{l}_1$
-	-	-	s	s	s	Z_3
-	-	-	s	s	a	$Z_3 \bar{c}_1$
-	-	-	s	a	s	$Z_3 \bar{c}_1$
-	-	-	s	a	a	$Z_3 \bar{c}_2$
-	-	-	a	s	s	$Z_3 \bar{c}_1$
-	-	-	a	s	a	$Z_3 \bar{c}_2$
-	-	-	a	a	s	$Z_3 \bar{c}_2$
-	-	-	a	a	a	$Z_3 \bar{l}_2$

the eigenvalues r in the case of working with Makhlin's and Jing's et al. invariants are listed in Tabs. I,II, and III. From these sets of projections it is apparent that we can learn the value of, e.g., optimal CHSH nonlocality by using fewer copies of $\hat{\rho}$ in the case of nonlocal HOM interferometers (see Fig. 7) than in the case of local HOM interferometers (see Fig. 6).

V. CONCLUSIONS

In this paper we studied two different sets of fundamental invariants of two-qubit states. We demonstrated how to perform direct measurements of Makhlin's and Jing's et al. invariants by applying HOM interference on multiple copies of the investigated two-qubit state. The developed techniques for designing such interferometers can be useful for designing new experiments for testing the quantum theory. We observed that W -state projections needed in direct measurements of some of the high order ($n = 10, 11, 15, 16, 17, 18$) invariants I_n solve a classical problem of deciding handedness much faster than any classical (local) strategy. Our analysis of Jing's et al. invariants also revealed that the nonlocal measurements or W -state projections are unnecessary for checking the equivalence of any two given two-qubit states. We demonstrated that by using nonlocal interferometers we learn the sign of I_1 , which is not possible with using only local interferometers. Learning this sign is an extra information gain appearing from different (nonlocal) connections in the same quantum circuit. This makes the nonlocal measurements more efficient for quantifying nonclassical correlations than the local ones in terms of the resources needed for such measurements.

Alice and Bob can learn the value of the sign of I_1 only by collaborating with each other, either by performing local or nonlocal measurements. For this reason this extra information gain in the case of the joint measurements performed by Alice and Bob could be useful in quantum information processing or communication tasks similar to quantum secret sharing [62], but in a way that is invariant to local unitary operations. Naturally, for testing fundamental physics of nonlocality one should perform only local measurements to avoid cyclic reference to nonlocality. However, the nonlocal interferometers in some scenarios can be more useful for quantitative measurements. We demonstrated the usefulness of nonlocal projections explicitly on the two examples of HOM interferometers designed to quantify CHSH nonlocality, linear entropy and fully-entangled fraction with only local or both local and nonlocal HOM interferometers. We compare these setups in context of measuring nonlocality in Tab. IV. Note that for all the method based on eigenvalues of \hat{R} the product of the number of copies and the number of measurement is constant and equals 12. Thus, the efficiency of these methods under perfect conditions would be the same and does not depend on the number of copies. The method based directly on finding singular values of the correlation matrix $\hat{\beta}$ seems to be the most experimentally efficient but it is at the same time the most mathematically complex. This means that the required calculations can be computationally intensive and require some hardware to perform them. The singular values are typically found by first solving the eigenproblem for $\hat{\beta}\hat{\beta}^T = \hat{R}$ [63]. Thus, the presented experimental methods based on eigenvalues of \hat{R} can be interpreted as quantum-hardware implementations of calculating functions of spectrum of $\hat{\beta}\hat{\beta}^T$ and they shift a part of the computational effort from postprocessing to the experiment. This gives a physical meaning to the abstract algebraic operations required for measuring such fundamental quantities as nonlocality M or fully-entangled fraction f , and other quantities defined via optimal measurements. This implies the existence of a trade off between the experimental complexity and computational complexity of the relevant measurements and their post-processing.

Acknowledgments

We thank Adam Miranowicz for stimulating discussions. K.B. acknowledges the support by the Polish National Science Centre under grant No. DEC-2013/11/D/ST2/02638 and support by the Czech Science Foundation under the project No. 17-10003S.

TABLE IV: The comparison of various methods for measuring Bell-CHSH nonlocality given by Eq. (10). Note that one can use various combinations of numbers of copies and measurements as some of the measurements can be performed in parallel (see Figs. 5-7).

method	copies	measurements	procedure
direct [26]	1	∞	all CHSH inequalities
$\hat{\beta}$ matrix	1	9	local
\hat{R} matrix	2	6	local
I_1, I_2, I_3	4	3	nonlocal
I_1, I_2, I_3	6	2	nonlocal
I_1, I_2, I_3	12	1	nonlocal
J_1, J_2, J_3	6	2	local
J_1, J_2, J_3	12	1	local

Appendix A: Detection events for the handness invariants

Note that all the W -states used in this paper are invariant under cyclic permutations. This fact can be used to group measurement outcomes. Our analysis of the expressions for Makhlin's invariants I_n for $n = 10, 11, 15, 16, 17, 18$ resulted in the complete list of the detection events depicted in Fig. 8.

- [1] M. Grassl, M. Rötteler, and T. Beth, *Phys. Rev. A* **58**, 1833 (1998).
- [2] J. Kempe, *Phys. Rev. A* **60**, 910 (1999).
- [3] Y. Makhlin, *Quantum Information Processing* **1**, 243 (2002).
- [4] R. C. King, T. A. Welsh, and P. D. Jarvis, *Journal of Physics A: Mathematical and Theoretical* **40**, 10083 (2007).
- [5] N. Jing, S.-M. Fei, M. Li, X. Li-Jost, and T. Zhang, *Phys. Rev. A* **92**, 022306 (2015).
- [6] L. Koponen, V. Bergholm, and M. M. Salomaa, *Quantum Info. Comput.* **6**, 58 (2006).
- [7] E. M. Rains, *IEEE Transactions on Information Theory* **46**, 54 (2000).
- [8] A. Osterloh and J. Siewert, *Phys. Rev. A* **86**, 042302 (2012).
- [9] H. A. Carteret, *Phys. Rev. Lett.* **94**, 040502 (2005).
- [10] K. Bartkiewicz, P. Horodecki, K. Lemr, A. Miranowicz, and K. Życzkowski, *Phys. Rev. A* **91**, 032315 (2015).
- [11] K. Bartkiewicz, J. c. v. Beran, K. Lemr, M. Norek, and A. Miranowicz, *Phys. Rev. A* **91**, 022323 (2015).
- [12] E. Schrödinger, *Math. Proc. Camb. Phil. Soc.* **31**, 555 (1935).
- [13] A. Einstein, B. Podolsky, and N. Rosen, *Phys. Rev.* **47**, 777 (1935).
- [14] R. Horodecki, P. Horodecki, M. Horodecki, and K. Horodecki, *Rev. Mod. Phys.* **81**, 865 (2009).
- [15] C. H. Bennett and S. J. Wiesner, *Phys. Rev. Lett.* **69**, 2881 (1992).
- [16] C. H. Bennett, G. Brassard, C. Crépeau, R. Jozsa, A. Peres, and W. K. Wootters, *Phys. Rev. Lett.* **70**, 1895 (1993).
- [17] M. Żukowski, A. Zeilinger, M. A. Horne, and A. K. Ekert, *Phys. Rev. Lett.* **71**, 4287 (1993).
- [18] A. K. Ekert, *Phys. Rev. Lett.* **67**, 661 (1991).
- [19] N. Gisin, G. Ribordy, W. Tittel, and H. Zbinden, *Rev. Mod. Phys.* **74**, 145 (2002).
- [20] W. Dür, H.-J. Briegel, J. I. Cirac, and P. Zoller, *Phys. Rev. A* **59**, 169 (1999).
- [21] M. Bula, K. Bartkiewicz, A. Černoč, and K. Lemr, *Phys. Rev. A* **87**, 033826 (2013).
- [22] E. Meyer-Scott, M. Bula, K. Bartkiewicz, A. Černoč, J. Soubusta, T. Jennewein, and K. Lemr, *Phys. Rev. A* **88**, 012327 (2013).
- [23] N. Gisin, S. Pironio, and N. Sangouard, *Phys. Rev. Lett.* **105**, 070501 (2010).
- [24] J. Bell, *Physics* **1**, 195 (1964).
- [25] J. S. Bell, *Speakable and Unsayable in Quantum Mechanics*, 2nd ed. (Cambridge University Press, 2004).
- [26] J. F. Clauser, M. A. Horne, A. Shimony, and R. A. Holt, *Phys. Rev. Lett.* **23**, 880 (1969).
- [27] N. Brunner, D. Cavalcanti, S. Pironio, V. Scarani, and S. Wehner, *Rev. Mod. Phys.* **86**, 419 (2014).
- [28] C. K. Hong, Z. Y. Ou, and L. Mandel, *Phys. Rev. Lett.* **59**, 2044 (1987).
- [29] F. A. Bovino, G. Castagnoli, A. Ekert, P. Horodecki, C. M. Alves, and A. V. Sergienko, *Phys. Rev. Lett.* **95**, 240407 (2005).
- [30] S. P. Walborn, P. H. S. Ribeiro, L. Davidovich, F. Mintert, and A. Buchleitner, *Nature (London)* **440**, 1022 (2006).
- [31] J.-S. Jin, F.-Y. Zhang, C.-S. Yu, and H.-S. Song, *Journal of Physics A: Mathematical and Theoretical* **45**, 115308 (2012).
- [32] K. Bartkiewicz, K. Lemr, A. Černoč, and J. Soubusta, *Phys. Rev. A* **87**, 062102 (2013).
- [33] K. Bartkiewicz, B. Horst, K. Lemr, and A. Miranowicz, *Phys. Rev. A* **88**, 052105 (2013).
- [34] Ł. Rudnicki, P. Horodecki, and K. Życzkowski, *Phys. Rev. Lett.* **107**, 150502 (2011).
- [35] Ł. Rudnicki, Z. Puchała, P. Horodecki, and K. Życzkowski, *Phys. Rev. A* **86**, 062329 (2012).
- [36] K. Bartkiewicz, K. Lemr, and A. Miranowicz, *Phys. Rev. A* **88**, 052104 (2013).
- [37] T. Tanaka, G. Kimura, and H. Nakazato, *Phys. Rev. A* **87**, 012303 (2013).
- [38] T. Tanaka, Y. Ota, M. Kanazawa, G. Kimura, H. Nakazato, and F. Nori, *Phys. Rev. A* **89**, 012117 (2014).
- [39] A. Miranowicz, K. Bartkiewicz, J. Peřina Jr., M. Koashi, N. Imoto, and F. Nori, *Phys. Rev. A* **90**, 062123 (2014).
- [40] K. Bartkiewicz, A. Černoč, K. Lemr, and A. Miranow-

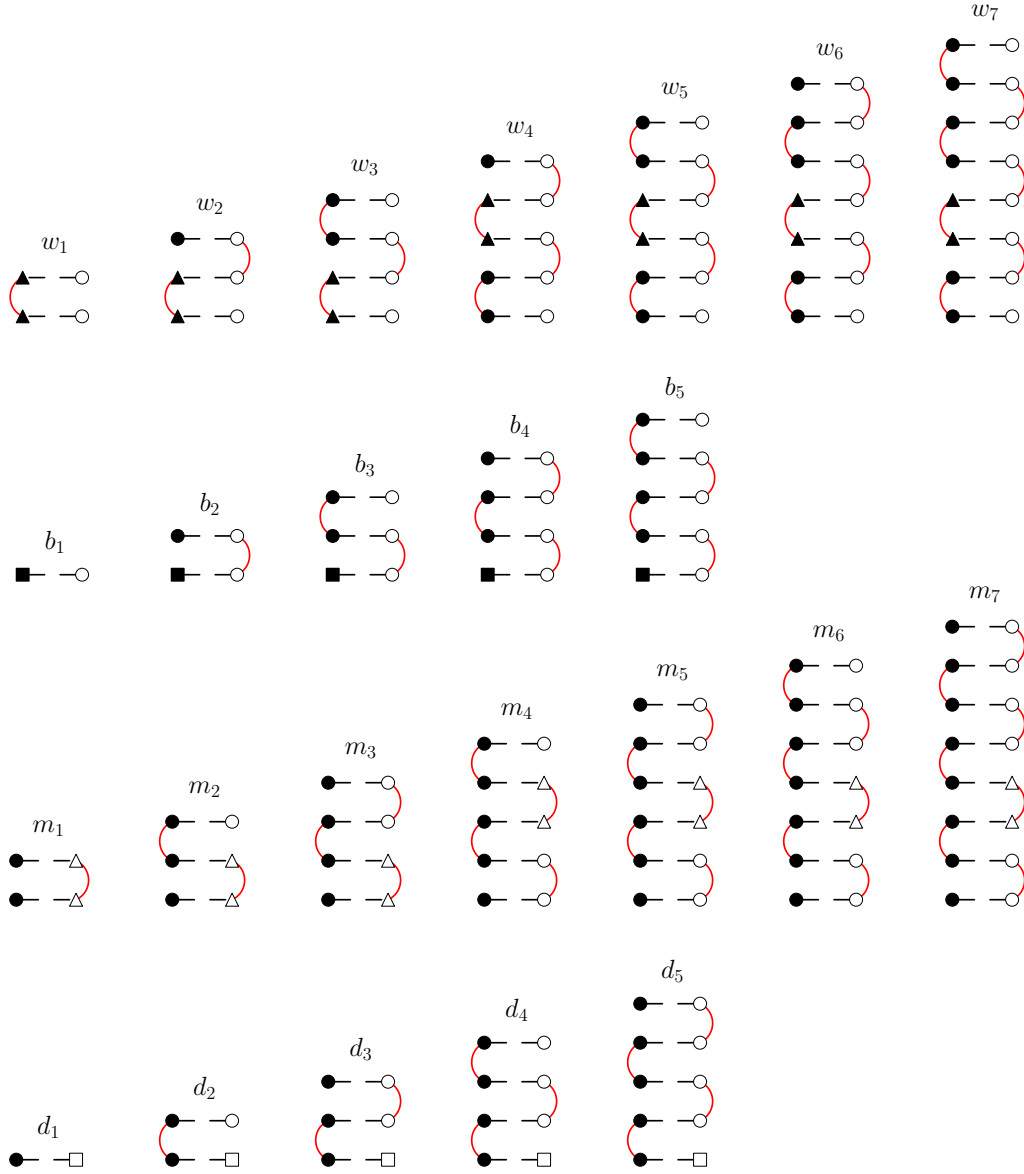


FIG. 8: The same as in Figs. 1 and 2, but for modified singlet projections (triangular markers) and $\hat{\sigma}_3$ measurements (square markers) involving W -state projections [see Eq. (6)] needed for determining the handedness invariants I_n for $n = 10, 11, 15, 16, 17, 18$.

- icz, Sci. Rep. , 19610 (2016).
- [41] K. Bartkiewicz, K. Lemr, A. Černoč, and A. Miranowicz, Phys. Rev. A **95**, 030102 (2017).
- [42] K. Lemr, K. Bartkiewicz, and A. Černoč, Phys. Rev. A **94**, 052334 (2016).
- [43] K. Bartkiewicz, G. Chimczak, and K. Lemr, Phys. Rev. A **95**, 022331 (2017).
- [44] J.-W. Pan, Z.-B. Chen, C.-Y. Lu, H. Weinfurter, A. Zeilinger, and M. Żukowski, Rev. Mod. Phys. **84**, 777 (2012).
- [45] W. Dür, G. Vidal, and J. I. Cirac, Phys. Rev. A **62**, 062314 (2000).
- [46] A. Aspect, P. Grangier, and G. Roger, Phys. Rev. Lett. **47**, 460 (1981).
- [47] A. Aspect, P. Grangier, and G. Roger, Phys. Rev. Lett. **49**, 91 (1982).
- [48] A. Aspect, J. Dalibard, and G. Roger, Phys. Rev. Lett. **49**, 1804 (1982).
- [49] R. Horodecki, P. Horodecki, and M. Horodecki, Phys. Lett. A **200**, 340 (1995).
- [50] R. Horodecki, Phys. Lett. A **210**, 223 (1996).
- [51] K. Bartkiewicz, B. Horst, K. Lemr, and A. Miranowicz, Phys. Rev. A **88**, 052105 (2013).
- [52] B. Hensen, H. Bernien, A. E. Dréau, A. Reiserer, N. Kalb, M. S. Blok, J. Ruitenber, R. F. L. Vermeulen, R. N. Schouten, C. Abellán, W. Amaya, V. Pruneri, M. W. Mitchell, M. Markham, D. J. Twitchen, D. Elkouss, *et al.*, Nature (London) **526**, 682 (2015).
- [53] L. K. Shalm, E. Meyer-Scott, B. G. Christensen, P. Bierhorst, M. A. Wayne, M. J. Stevens, T. Gerrits, S. Glancy, D. R. Hamel, M. S. Allman, K. J. Coakley, S. D. Dyer, C. Hodge, A. E. Lita, V. B. Verma, C. Lambrocco, *et al.*,

- Phys. Rev. Lett. **115**, 250402 (2015).
- [54] C. H. Bennett, D. P. DiVincenzo, J. A. Smolin, and W. K. Wootters, Phys. Rev. A **54**, 3824 (1996).
- [55] R. Horodecki and M. Horodecki, Phys. Rev. A **54**, 1838 (1996).
- [56] D. Grondalski, J. and Etlinger and D. James, Phys. Lett. A **300**, 573 (2002).
- [57] P. Badziag, M. Horodecki, P. Horodecki, and R. Horodecki, Phys. Rev. A **62**, 012311 (2000).
- [58] T. Tashima, Ş. K. Özdemir, T. Yamamoto, M. Koashi, and N. Imoto, Phys. Rev. A **77**, 030302 (2008).
- [59] T. Tashima, Şahin Kaya Özdemir, T. Yamamoto, M. Koashi, and N. Imoto, New Journal of Physics **11**, 023024 (2009).
- [60] T. Tashima, T. Kitano, Ş. K. Özdemir, T. Yamamoto, M. Koashi, and N. Imoto, Phys. Rev. Lett. **105**, 210503 (2010).
- [61] M. Horodecki, P. Horodecki, and R. Horodecki, Phys. Lett. A **223**, 1 (1996).
- [62] M. Hillery, V. Bužek, and A. Berthiaume, Phys. Rev. A **59**, 1829 (1999).
- [63] K. F. Riley, M. P. Hobson, and S. J. Bence, *Mathematical methods for physics and engineering: a comprehensive guide* (Cambridge university press, 2006).